ECS Transactions, 72 (7) 215-224 (2016)
10.1149/07207.0215ecst ©The Electrochemical Society

Time Resolved DXAS Study on Micro and Nano NiO/$Ce_{0.9}Gd_{0.1}O_{1.95}$ Cermets for Intermediate Temperature Solid Oxide Fuel Cells

A. Fernandez Zuvich[a], S. Larrondo[b], M. E. Saleta[c], F. R. Napolitano[a,d], A. Caneiro[a,d], H. E. Troiani[a,d], D.G. Lamas[d,e], M. D. Arce[a,d], A. Serquis[a,d] and A. L. Soldati[a,d]

[a] CONICET, CAB-CNEA, Av. Bustillo 9500, S. C. de Bariloche, R8402AGP, Argentina
[b] Centro de Investigaciones en Sólidos (CINSO-CITEDEF-UNIDEF-CONICET), Buenos Aires, B1603ALO, Argentina
[c] Instituto de Física "GlebWataghin", UNICAMP, Campinas-SP 13083-859, Brazil.
[d] CONICET, Argentina.
[e] Escuela de Ciencia y Tecnología, UNSAM, San Martín, Argentina.

We present a crystallographic, morphologic and redox dynamic study on (60:40) NiO/$Ce_{0.9}Gd_{0.1}O_{1.95}$ (NiO/GDC) cermets simulating Intermediate Temperature Solid Oxide Fuel Cells (IT-SOFC) anodes *in situ* conditions. We tested micro- and nanometer sized materials at 700ºC in three different atmospheres (5% H_2, 5% O_2 and 20% CH_4). We used Dispersive X-ray Absorption Spectroscopy (DXAS) analysis at the Ce L_3-edge and at the Ni K-edge to follow the metal´s oxidation states. A correlation between the catalytic/redox properties and the sample´s characteristics (microstructure, Ni distribution, etc.) was found, indicating that nanometric sized particles showed faster and higher reduction extents than micrometric particles of the same composition.

Introduction

CeO_2-based materials present excellent catalytic properties for the oxidation of H_2 and CH_4 fuels (1) and therefore they are considered as candidates for Intermediate Temperatures Solid Oxide Fuel Cells (IT-SOFC) anode materials (2). Although they lack of appropiate electronic conductivity, it could be improved by the addition of metals such as Ni, enabling them as efficient IT-SOFC anodes (3). Several chemical routes have been used to produce this kind of anodes in order to obtain different microstructures and morphologies varying the synthesis method, as well as the way the metal is incorporated into the material (4).

The effect of the material's characteristics on the electrocatalytic activity of the anode towards different fuels is not fully understood. In order to elucidate this point, in the present work, a modified sol-gel route was used to prepare samples varying sintering temperatures in order to obtain different characteristic grain sizes and microstructures. The reaction kinetics of these samples were studied by *in situ* time resolved Dispersive X-ray Absorption Spectroscopy (DXAS) under two reducing atmospheres (5% H_2/He and 20% CH_4/He) at 700ºC and allowing an intermediate re-oxidation in 5% O_2/He at the same temperature. The results were compared with a commercial cermet sample.

Materials and Methods

Synthesis of mixed oxides

Nanostructured cermets of composition 60% w/w NiO - 40% w/w $Ce_{0.9}Gd_{0.1}O_{1.95}$ (NiO/GDC) were synthesized through a modified sol/gel method, using $Ce(NO_3)_3.6H_2O$, Gd_2O_3 and $Ni(NO_3)_2.6H_2O$ as precursors and thermally treated at 350ºC for 2 hours (currently under patent process, details will be published elsewhere). Then, the anode material (labelled as 'A'), was uniaxially pressed into pellets and sintered at two different temperatures, 900 ºC and 1350 °C for 1 hour (See Table 1). In addition, pellets of a commercial cermet from Fuel Cell Materials® (labelled as 'C') with the addition of 7.5% activated carbon (5) were prepared and sintered at 1350ºC for 1 hour for comparison. After this heat treatment, the pellets were milled and characterized by different techniques.

X-ray Powder Diffraction

The present phases, crystallite size and lattice strain of samples were studied by Synchrotron and laboratory X-ray powder diffraction (XPD). Synchrotron experiments were performed at LNLS D10B-XPD beamline with 8 keV photon energy (1.55 Å) using a Hubber 4+2 circle diffractometer (6), and a Mythen1K detector placed at 935 mm from the sample. Laboratory experiments were carried out with a PANalytical Empyrean X-ray diffractometer with CuKα radiation, graphite monochromator and a PIXcel 3D detector. Diffractograms were collected in the $20° < 2\theta < 90°$ region. The data were treated with the X'Pert© Software.

Scanning and Transmission Electron Microscopy

The cermet´s microstructure was studied with a FEI Nano-Nova Field Emission Gun - Scanning Electron Microscope (FEG-SEM) equipped with an EDAX Genesis 2000 spectrometer for Energy Dispersive Spectroscopy (EDS) microanalysis. Additionally, Transmission Electron Microscopy (TEM) images were obtained using a Philips CM 200 UT microscope equipped with a LaB_6 filament operated at 200 keV and ultra-twin objective lens. For TEM preparation, particles were dispersed in isopropanol, ultrasonicated for 5 min and deposited in Cu/hollow Carbon TEM grids.

Dispersive X-ray Absorption Spectrometry

Oxidation state evolution of Ce and Ni in the samples was measured by Dispersive X-ray Absorption Spectroscopy at the D06A-DXAS beamline of the Brazilian Synchrotron Light Laboratory (LNLS, Campinas, Brazil: Proposal DXAS-XAFS1–16192). This beamline is equipped with a Si (111) monochromator and a CCD detector. About 3 spectra per minute were acquired, within a range of 80 eV before and 120 eV after for both Ce L_3 and Ni K absorption edges. CeO_2, $CeOHCO_3$, Ce $(NO_3)_3$, NiO and Metallic Ni were used as standards for oxidation states and for energy calibration.

The NiO/GDC samples were mixed together with BN in a w/w ratio 1:10 and pressed into self-supporting pellets using a uniaxial press. Typically, 10 mg of sample was used to form the pellet, which produced a total absorption ratio of 1.5. Afterwards, the pellets were mounted in a home-made quartz oven that allowed temperature and gas flux control. *In situ*

X-ray Absorption Near Edge Spectroscopy (XANES) studies were performed simulating the SOFC operating conditions as anode under Hydrogen and Methane rich atmospheres, allowing an intermediate step for re-oxidation between both reducing cycles.

The samples were first treated under 5% H_2/He, following a heating rate of 10ºC.min^{-1} from room temperature up to 700°C, followed by a dwell time of 2 hours for stabilization purposes. After that, keeping constant temperature at 700ºC, the gas flux was changed to 20% O_2/He for another two hours to allow re-oxidation. Finally, the samples were reduced under 20% CH_4/He for 30 minutes at the same temperature (See Figure 1).

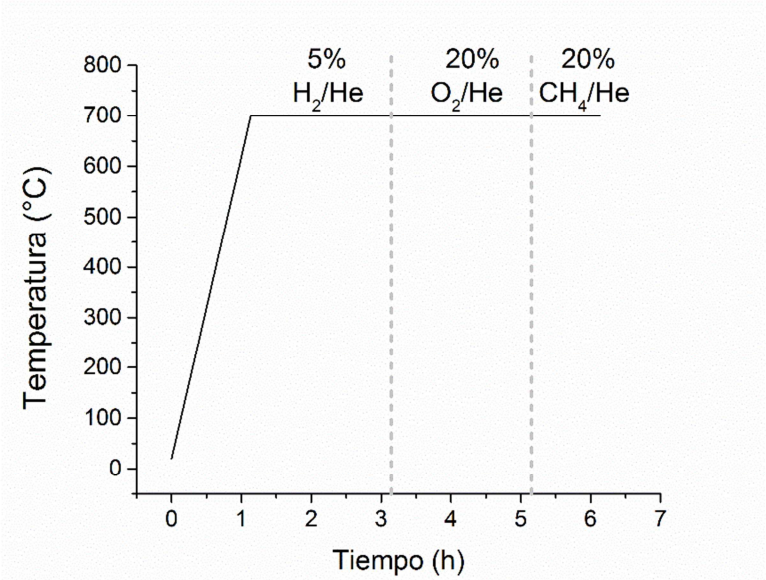

Figure 1: Thermal treatment applied to simulate in situ conditions as SOFC anode under H_2 and CH_4 atmospheres. A re-oxidation step was introduced between both reductions at 700ºC. Between gas changes, He was used to purge the reactor and feed lines.

The spectra were normalized using the data treatment program Prestopronto© (7) and principal components analysis (PCA) was performed using its PCA-GUI module. This tool statistically analyses a large quantity of spectra (around 1000 per sample), identifying (through an orthogonal transformation) linearly uncorrelated variables, which are called the principal components or eigenfunctions. Their linear combination accounts, thus, for the observed variance of the data. In this work, because of physical reasons, only the first two components (with the higher eigenvalues) were selected for the analysis.

In most of the cases, the two principal components obtained by PCA were undoubtedly different and correspond to the most oxidized and the most reduced spectra obtained at each run. It is worth to mention at this point that the principal components of Ce-measurements coincide with Ce^{4+} spectra but not with Ce^{3+} spectra (See Figure 5a). This fact indicates that in all cases, the reduction of Ce^{4+} to Ce^{3+} was not 100%. The values shown by PCA are not absolute but represent the degree of reduction of the samples. Indeed, this data treatment serves to compare the reduction process kinetics between the samples (8).

Electrochemical Impedance Spectroscopy

Area Specific Resistance (ASR) anode values were determined in symmetrical cells from Electrochemical Impedance Spectroscopy measurements (EIS) under Ar/H2 (95% at - 5 at %) mixture, carried out heating from 500 to 700 °C (50 °C steps), as described elsewhere (5). Anode films were prepared as inks and deposited by spin-coating method on GDC dense pellets. A rotation speed of 4000 rpm for 20 seconds was used, forming a layer of uniform thickness. Symmetrical cells (anode / electrolyte / anode) were obtained after a heat treatment to achieve good adhesion between layers (sintering at 1000 ° C for 12 hours).

Results and Discussion

Morphology and Microstructure Characterization

SEM and TEM micrographs of samples sintered at 900ºC and 1350ºC are shown in Figure 2. As expected, the influence of sintering temperature in the morphology is clearly observed; sample sintered at 900ºC present grain size two orders of magnitude smaller than those sintered at 1350ºC. In addition, samples synthesized by the sol-gel route have a homogeneous distribution of GDC and NiO particles. Furthermore, GDC and NiO particles present approximately the same sizes with no clear morphological differences between both phases. On the other hand, the commercial sample (C1350) shows smaller NiO particles (identified by EDS) than those corresponding to the GDC phase.

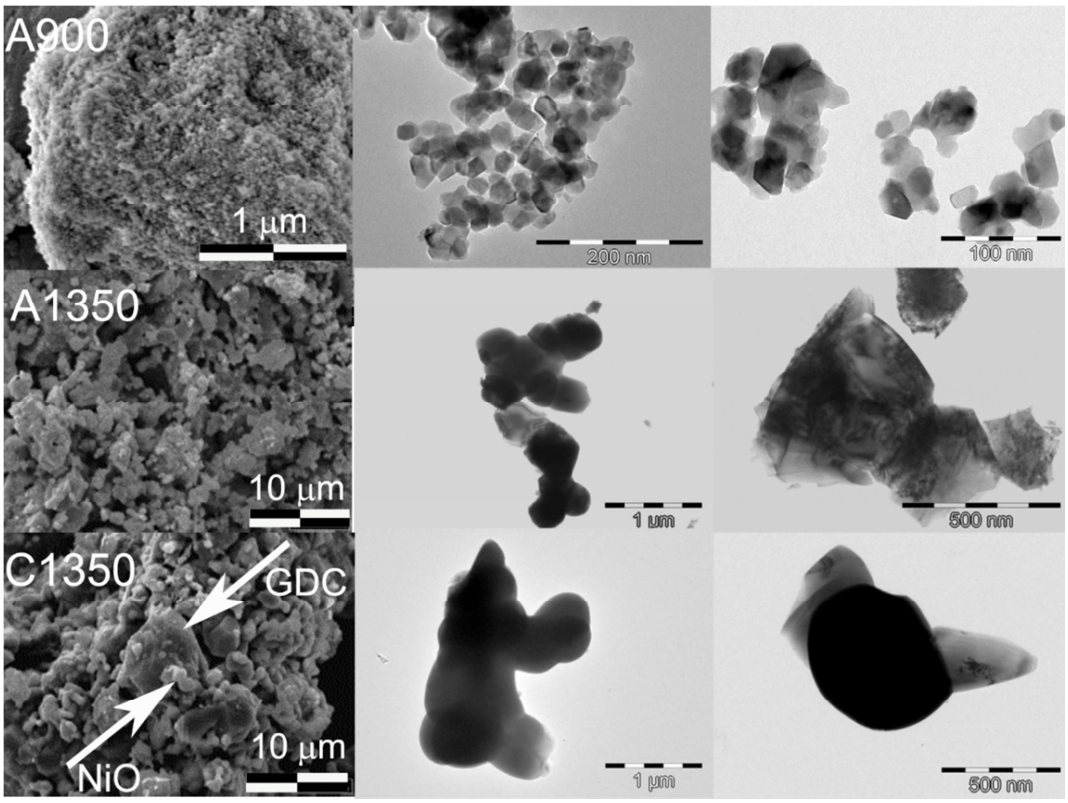

Figure 2. SEM (left) and TEM (middle and right) micrographs of anode samples sintered for 1h at 1350°C and 900ºC showing the nanostructure obtained by the modified sol-gel route in comparison to the commercial cermet sintered at 1350ºC (C1350).

Crystal phases and crystallinity

X-ray diffractograms of the commercial and the sol-gel samples (Figure 3a) at the beginning of the experiment present the main reflections of GDC and NiO cubic crystals (both belonging to Fm3m space group) as separated phases. The initial powders A_0 and C_0 were measured previous to the thermal treatments and the diffractograms are shown in Figure 3a. Contrary to A_0, the commercial powder C_0 presents narrow peaks, indicating larger grain sizes. Indeed, the crystallite sizes calculated by Scherrer equation (X' Pert High Score Plus) demonstrate that average crystallite size on C_0 is two order of magnitude larger than those synthetized by our own method (Table I). Figure 3b shows the present phases after the thermal treatment. The average crystallite size size obtained from these diffractograms are shown in Table I. Sample A900 resulted in smaller crystallite sizes than samples A1350 and C1350, as expected from a lower sintering temperature. The X-ray results are in agreement with those of SEM, EDS and TEM.

TABLE I. Sample characteristics, including crystallite sizes and lattice strain determined by XPD.

	Sample name	Thermal treatment (ºC)	Crystallite Size (nm)		Lattice strain (%)	
			GDC	NiO	GDC	NiO
Sol-gel	A0	-	3	11	2,0	0,8
	A900	900	35	39	0,2	0,2
	A1350	1350	207	168	0,1	0,1
Commercial	C_0	-	107	182	0,1	0,1
	C1350	1350	789	310	0,04	0,1

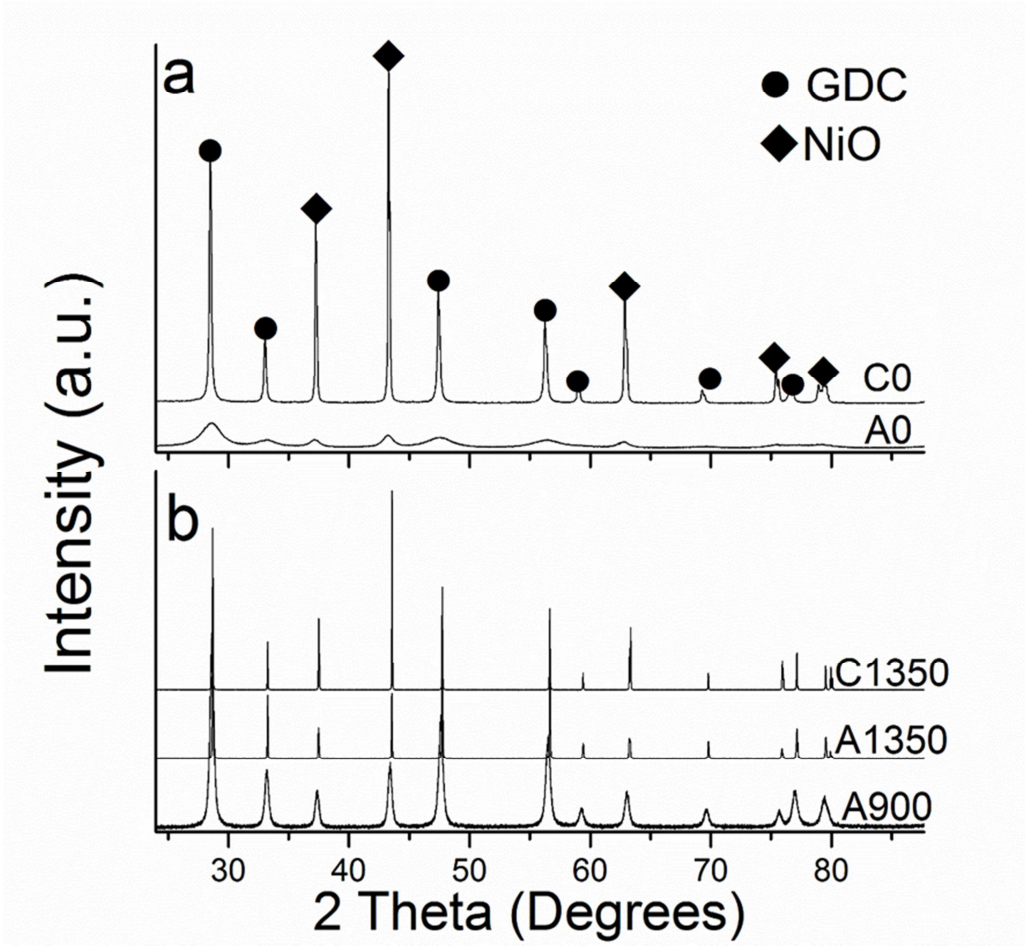

Figure 3: X-ray diffractograms of the initial samples (a), and sintered at 900 and 1350ºC (b).

Synchrotron XPD results for a nanoparticulated sample and for the commercial sample are shown in Figure 3. All peaks identified belong to Ni, NiO and $Ce_{0.9}Gd_{0.1}O_{2-\delta}$. No other crystalline phase is observed.

Characterization of atomic species during reduction and re-oxidation process

X-ray absorption spectrum at Ce L_3 and Ni K edges region were acquired *in situ* during the thermal treatments with a sampling frequency of about three spectra per minute. The components found by PCA could be recognized in Ce^{4+} / Ce^{3+} and Ni^{2+} / Ni^0 typical X-ray absorption spectra. This fact was also verified by measuring different reference materials at room temperature (Figure 4). For example, the most oxidized spectrum of A900 (A900_ox) presents the characteristic double absorption peak of the CeO_2 reference, while the most reduced one (A900_red) is a mixture between the Ce^{3+} and the Ce^{4+} reference patterns (Figure 4a). A similar analysis can be done for the two Ni components although, contrary to the Ce case, Ni oxide and metallic reference materials represent clearly the same spectral features than the oxidized and reduced cermets, respectively (Figure 4b).

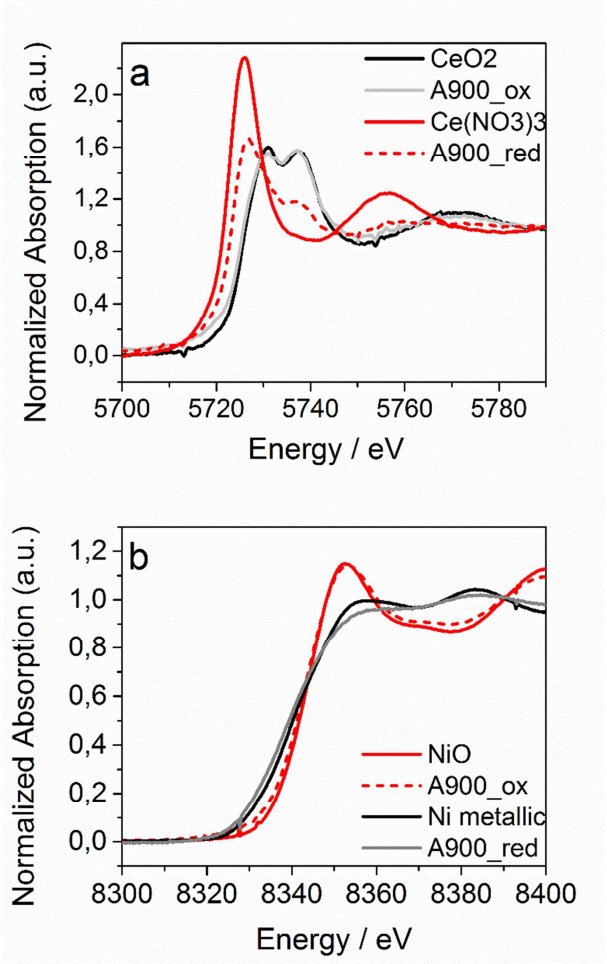

Figure 4: XANES spectra of Ce and Ni reference materials and sample A900. (a) Ce L_3-edge showing the Ce^{3+}($Ce(NO_3)_3$) and Ce^{4+} (CeO_2) reference spectra and sample A900 in its most reduced (A900_red) and its most oxidized (A900_ox) states. (b) Ni K-edge showing the Ni^{2+} (NiO) and Ni^0 (Ni Metallic) reference spectra and sample A900 in its most reduced (A900_red) and its most oxidized (A900_ox) states.

The evolution of the oxidized and reduced species in samples C1350, A1350 and A900, are displayed in Figure 5 (Ce L_3 edge) and 6 (Ni Kedge). At this point it is worth to mention that the Ni spectra of sample C1350 at 700°C are all very similar regardless of the atmosphere, thus the PCA method failed in calculating the principal components. Therefore, this data is not shown in Fig. 6.

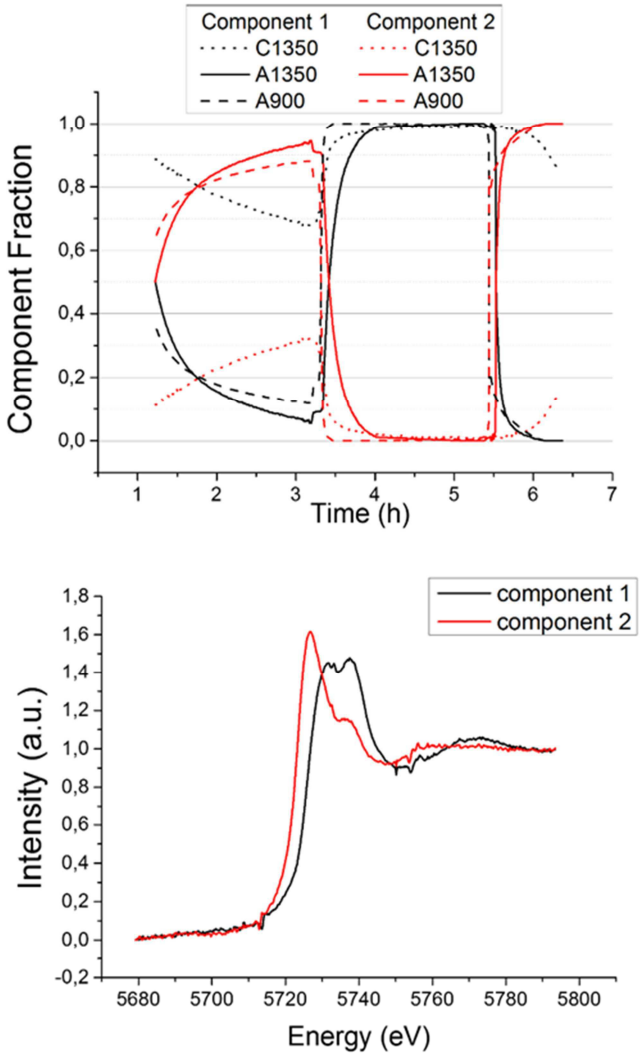

Figure 5: (a) PCA Ce response for samples sintered at 900 and 1350. (b) Eigenfunctions used to calculated (a)

The calculation of Ce edge in DXAS measurements reveals that A1350 and A900 are more reactive than C1350 under both reducing atmospheres (5% H_2 and 20% CH_4). During the oxidation treatment under O_2 at 700ºC, A900 reacts almost instantaneously to the atmosphere change transforming all Ce into Ce^{4+} while A1350 and C1350 need a stabilization time of 0.5 hours. In the CH_4 atmosphere, A900 and A1350 are clearly faster than C1350 and react immediately after the atmosphere change, stabilizing after some minutes. Moreover, C1350 presents a slow kinetic of reaction, without reaching a stable state at the end of the experiment.

Regarding the Ni K-edge measurements, faster kinetic response could be observed for the nanometric sample under 5% H_2 or 5% O_2 atmospheres. On the other hand, under a CH_4 rich atmosphere, both samples react immediately requiring only some minutes to stabilize to metallic Ni.

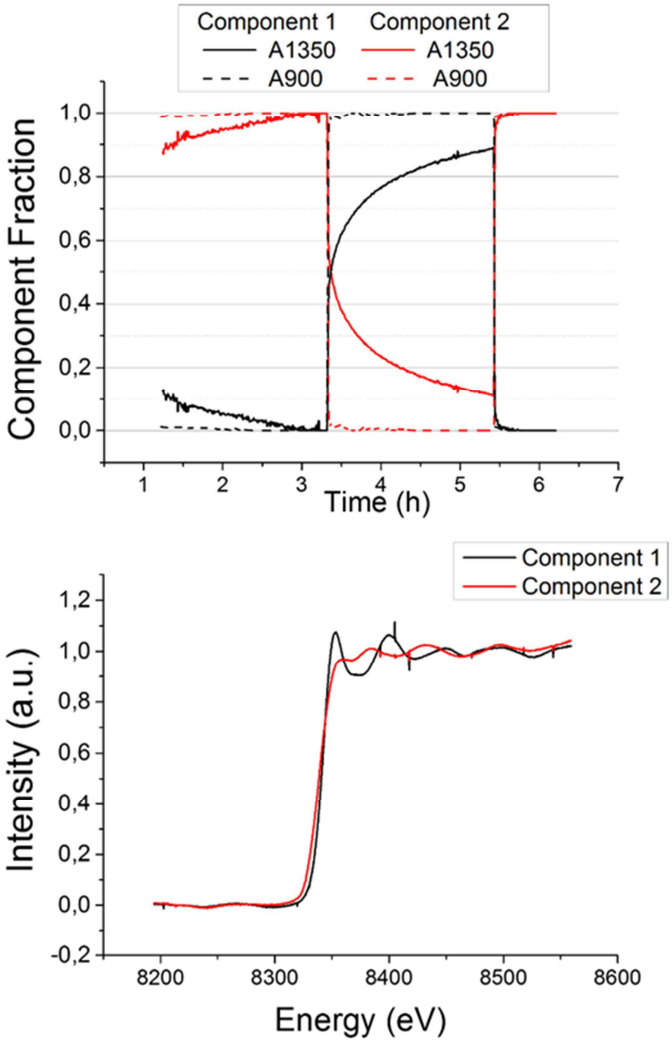

Figure 6: (a) PCA Ni response for samples sintered at 900 and 1350. (b) Eigenfunctions used to calculated (a)

EIS measurements under an Ar/H_2 atmosphere show better results for the sol-gel samples compared to those anodes prepared with the commercial powders at the same conditions. The Area Specific Resistance (ASR) resulted in more than one order of magnitude larger for sample C1350 than the ASR values of A1350 (0.134 ohm.cm^2 for the first one and 0.0036 ohm.cm^2 for the later one at 650°C -see Figure 7-). On the other hand ASR values of the commercial sample at 600-700° range were only three times larger than those of sample A900.

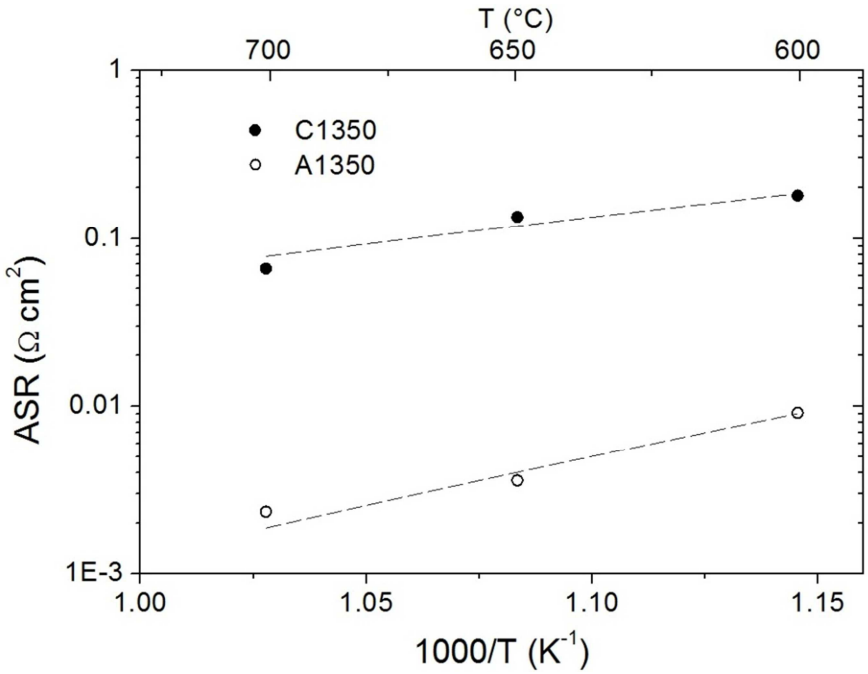

Figure 7: Area Specific Resistence (ASR) as a function of temperature for commercial and synthesized NiO/GDC anodes under Ar/H_2 atmosphere. The dotted lines represent the linear fitting of the values.

Conclusions

Nanostructured NiO/GDC powders were synthesized using a modified sol-gel method in order to obtain different IT-SOFC anodes morphologies with nanometre grain sizes. The resulting materials were characterized by XPD, SEM, TEM, DXAS and EIS. Initially, the samples have two separated phases NiO and GDC with cubic crystal phase (*Fm3m* space group) presenting crystallite sizes in the nanometric range, depending on the sintering temperature. DXAS time resolved experiments simulating *in situ* conditions as IT-SOFC anode helped to evaluate the ratio between the oxidized and the reduced species for Ni and Ce using H_2 and CH_4 as fuels. In addition, the reduction kinetic studies showed that smaller grain size samples (sintered at 900ºC) behave very similar, although faster, than those with bigger grain sizes.

Acknowledgments

This work was supported by ANPCyT (Argentina, PICT-2010-00322), CONICET (Argentina, PIP 2012 112-201101-00366), Universidad Nacional de Cuyo (Argentina, Project 06/C447), CNEA and LNLS (Brazil, Research Proposal #16192 D06A-DXAS beamline), and the BMBF-MinCyT Bilateral Collaboration (Project AL1013). The authors thank Dr. Santiago Figueroa for his support with the PCA program.

References

1. A. Trovarelli, *Catalysis Reviews - Science and Engineering*, **38**(4), 439 (1996).
2. M. Mogensen, S. Primdahl, M. J. Jørgensen and C. Bagger, *Journal of Electroceramics*, **5**(2), 141 (2000).
3. C. Xia and M. Liu, *Solid State Ionics*, **152-153**, 423 (2002).

4. N. Mahatoa, A. Banerjeea, A. Guptaa, S. Omarc and K. Balani, *Progress in Materials Science*, **72**, 141 (2015).
5. A. Fernandez Zuvich, A. Caneiro, C. Cotaro and A. Serquis, *Procedia Materials Science*, **1**, 628 (2012).
6. F. F. Ferreira, E. Granado, W. Jr. Carvalho, S. W. Kycia, D. Bruno and R. Jr. Droppa, *Journal of Synchrotron Radiation*, **13**(1), 46 (2006).
7. C. Prestipino and S. J. A. Figueroa, *PrestoPronto*. 2010: http://soonready.github.io/PrestoPronto/
8. M. G. Zimicz, S. A. Larrondo, R. J. Prado and D. G. Lamas,. *International Journal of Hydrogen Energy*, **37**(19), 14881 (2012).
9. PANalytical, *X'pert HighScore Plus* 2011.